Bandwidth Enhancement of Circularly Polarized Dielectric Resonator Antenna

Ru-Ying Sun

Axial-ratio (AR) bandwidth enhancement is achieved for a circularly polarized (CP) cylindrical dielectric resonator antenna (DRA) using a wideband hybrid coupler (WHC) combined with dual probe feed. The presented WHC, comprised of a Wilkinson power divider and a wideband 90° shifter, delivers good characteristics in terms of 3 dB power splitting and consistent 90° (±5°) phase shifting over a wide bandwidth. In turn, the proposed CP DRA, for the employment of the WHC, in place of conventional designs, provides a significant enhancement on AR bandwidth and impedance matching. The antenna prototype with the WHC exhibits a 3 dB AR bandwidth of 48.66%, an impedance bandwidth of 52.5% for voltage standing wave ratio (VSWR) ≤ 2, and a bandwidth of 44.66% for a gain of no less than 3 dBi. Experiments demonstrate that the proposed WHC is suitable for broadband CP DRA design.

Keywords: Circularly polarized antenna, dielectric resonator antenna, wideband hybrid coupler, axial ratio bandwidth.

I. Introduction

The dielectric resonator antenna (DRA) has been widely investigated and used over the last two decades since it was introduced in 1983 [1]–[2]. This is because the DRA offers many attractive features, such as high radiation efficiency, ease of excitation, and a relatively wide impedance bandwidth compared with microstrip antennas. Moreover, its size and bandwidth can be easily controlled by the dielectric constant of the material over a wide range [3]. The wideband circularly polarized (CP) antenna has been widely employed in many applications including radio-frequency identification (RFID), radar, satellite, and mobile telecommunication. In satellite communications, for instance, the circular polarization is used to overcome the polarization rotation effects due to the atmosphere. Radar systems use CP waves to obain more information from targets. Generally, CP systems allow for more flexibility in orientation of the transmitter and the receiver antennas [4]. Therefore, a good number of efforts have been focused on CP DRAs in recent years [5]–[19].

The feed schemes of CP DRAs are normally divided into two categories: single feed and dual/multiple feed [2]. For the CP DRAs with simple-structure dielectric resonators (DRs), the single-feed type [5]–[13] usually has a relatively narrow 3 dB axial-ratio (AR) bandwidth in the range of 3% to 10% for $\varepsilon_r \approx 10$ [5]–[7]. In recent years, significant efforts have been made to improve AR bandwidths for single-feed CP DRA. Radiating with a stair-shaped DR [8] and feeding with a square spiral strip [9]–[10] are both efficient ways to increase AR bandwidths in the order of 10% to 25%. In addition, wider bandwidth for the single-feed type can be achieved using super-shaped DRs [11]–[13]. However, it is not easy to obtain these irregular DRs commercially on account of their complex

Manuscript received May 24, 2014; revised Aug. 18, 2014; accepted Sept. 29, 2014.

Ru-Ying Sun (srysd@163.com) is with the Department of Electrical Engineering, the School of Automobile Engineering, Linyi University, Shandong, China.

geometry and the corresponding high cost of fabrication.

For the flexibility of the feed network design and the utility of the simple-structure DR, dual/multiple-feed CP DRAs are attractive in wideband applications. In the approaches [14]–[19], hybrid couplers are often used to generate quadrature feeding signals, with which the CP DRAs usually provide much wider AR bandwidths than the single-feed type. A dual-probe feed CP DRA with a 3 dB quadrature coupler can achieve 2 dB AR bandwidth of 11% (3 dB AR bandwidth is not given) for $\varepsilon_r = 36.2$ [14]. For lower relative permittivity ($\varepsilon_r \sim 10$), more than 20% 3 dB AR bandwidths can be obtained for dual/multiple-feed CP DRAs fed by fundamentally designed quadrature couplers [15]–[19]. However, the effective AR bandwidth of the CP DRA with conventional quadrature couplers [15]–[19] is limited to 25.9%, even though the antenna has a sequentially rotated feed with a quadruple conformal strip [16]. This limitation may have come from its coupler, whose bandwidth is limited by the frequency dependence of the quarter-wavelength transmission line and is generally of the order of 20% to 30% [20].

In [21], it has been proved that the antenna CP bandwidth is frequency independent, while the phase and magnitude of the quadrature signals are frequency independent. Therefore, the high-performance quadrature coupler on phase shifting and impedance matching is a candidate for broadband CP design as far as the DRA itself can provide the two quadrature signals. In this paper, a novel wideband hybrid coupler (WHC) is proposed for the wideband CP DRA design. The CP DRA with the WHC demonstrates enhanced wideband characteristics in terms of circular polarization and impedance matching. The simulations and experiments on the presented CP DRA have been taken to validate the design strategy, including the results of the voltage standing wave ratio (VSWR), AR bandwidth, antenna gain, and radiation patterns.

II. Antenna Configuration and Design

The configuration of the proposed antenna with the WHC is shown in Fig. 1. The DR with a low relative permittivity $\varepsilon_{rd} = 10.0$ has a circular cross-section, which is located at the center of the substrate. The substrate is Rogers RT/duroid 6002 with thickness $t = 0.508$ mm and relative permittivity $\varepsilon_{rs} = 2.94$, and it has the same dimension as the ground plane, occupying an area of $L \times L = 43$ mm $\times$ 43 mm. The feed network, comprised of a 3 dB Wilkinson power divider and a wideband 90° shifter, is printed on the back of the substrate and is investigated in more detail below.

To achieve dual-feed-type circular polarization, a pair of orthogonally-orientated vertical probes connected to the WHC is employed to excite the DR at the furthest point from the DR

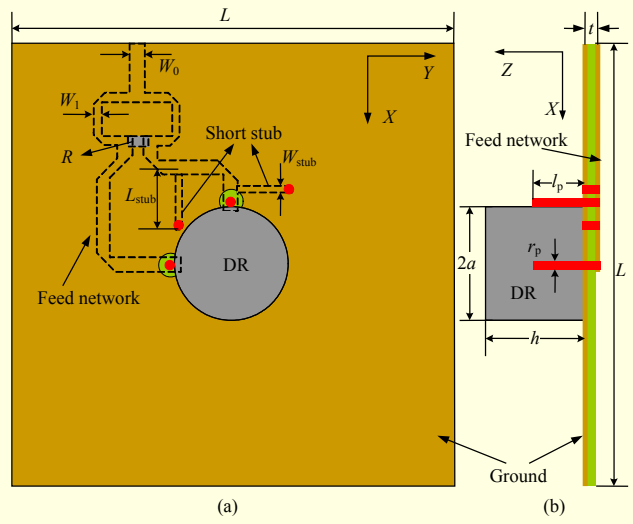

Fig. 1. Configuration of proposed antenna with WHC: (a) top view and (b) side view.

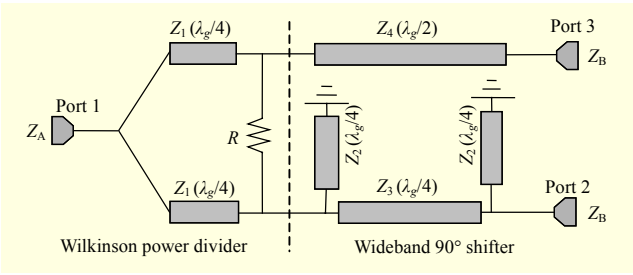

Fig. 2. Schematic of WHC.

axis, and the corresponding two quadrature signals are then generated. Good impedance matching can be achieved by adjusting the probe dimensions — the diameter (r_p) and height (h_p).

Figure 2 shows a schematic of the proposed WHC, which consists of a Wilkinson power divider and a wideband 90° shifter. The divider achieves not only power division but also impedance transforming between input and output ports. It is seen that the input signal at Port 1 is split into two paths through a pair of quarter-wavelength transformers, and then they transmit along the paths generating 90° phase difference at output ports 2 and 3 because of the 90° shifter. The main component of the WHC is the wideband 90° shifter, which is a simplified design from the shifter in [22]. The proposed wideband 90° shifter is comprised of a reference transmission line Z_4 ($\lambda_g/2$) and a transmission line Z_3 ($\lambda_g/4$), of which two short stubs Z_2 ($\lambda_g/4$) are shunted at both ends. The short stubs are employed to smooth the phase change and match the impedance over the desired bandwidth between the input and output ports. The 90° shifter in [22] consists of an open stub and a short stub; a main transmission line with a half wavelength; and a corresponding reference transmission line

with three-quarter wavelength. Therefore, the proposed 90° shifter is more compact than the reference shifter.

As a design guideline, formulae (1)–(4) (below) are presented for the proposed feed network in a general way, where Z_A and Z_B stand for the impedance at the input port and two output ports, respectively. The characteristic impedance of the different transmission lines is represented by Z_i ($i = 1, 2, 3, 4$).

$$R = 2Z_B, \tag{1}$$

$$Z_1 = \sqrt{2Z_A \cdot Z_B}, \tag{2}$$

$$Z_2 = 1.52Z_B, \tag{3}$$

$$Z_3 = Z_4 = Z_B. \tag{4}$$

To demonstrate the methodology mentioned above, the WHC is operated at a central frequency of 6.0 GHz. For convenience, the characteristic impedance of both the input and output ports of the WHC are assumed to be 50 Ω. The parameters of the WHC are as follows: $Z_1 = 70.7$ Ω, $Z_2 = 76$ Ω, $Z_3 = Z_4 = Z_A = Z_B = 50$ Ω, and $R = 100$ Ω. The simulations of the WHC are carried out using the full-wave software ANSYS High Frequency Structure Simulator (HFSS) 15.0. The amplitude and phase responses of the WHC are shown in Fig. 3. With reference to the figure, the WHC exhibits wideband characteristics in terms of equal power splitting and 90° phase shift. The responses indicate an operating bandwidth of 47.58% for $S_{11} \leq -15$ dB and consistent 90° phase shift with a deviation of ±5°. The WHC achieves much wider bandwidth than those of the conventional feed networks used in [15]–[19].

To explain the AR bandwidth enhancement in more detail, the effect of the short stubs in the feed network is investigated by studying two antennas — the reference CP antenna (without short stubs) (I) and the proposed CP antenna II. Their configurations are illustrated in Fig. 4, and Fig. 5 shows their

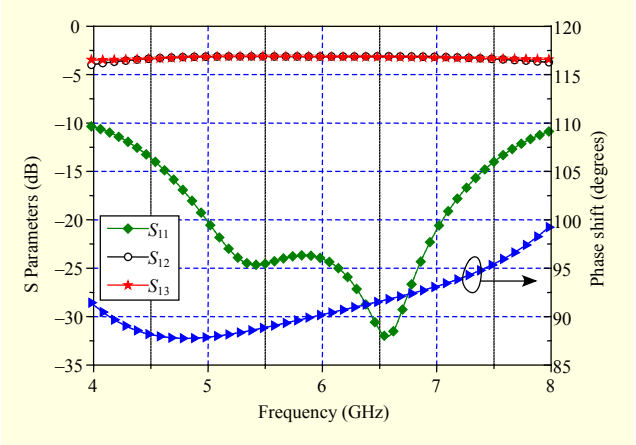

Fig. 3. Simulated amplitude and phase responses of WHC.

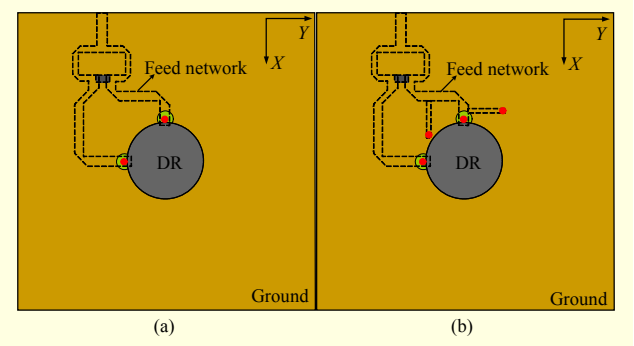

Fig. 4. Configurations of reference antenna and proposed antenna: (a) antenna I and (b) antenna II.

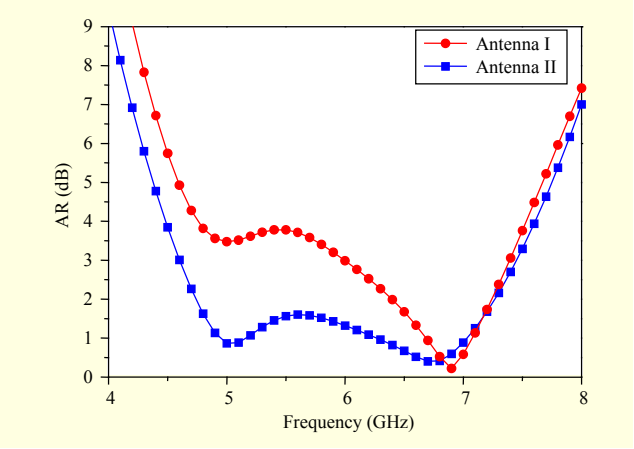

Fig. 5. Simulated ARs of antenna I and antenna II.

corresponding ARs. The dimensions of the two antennas are basically the same as for the present design, except that antenna I has no short stubs.

With reference to Fig. 5, both antennas can generate CP fields. Also, it is apparent by comparing the two curves that the lower AR passband of antenna II is caused by the short stubs. When the short stubs are added to the feed network, there is an interaction between them, and consequently, a wideband CP performance for antenna II is achieved.

A parametric study of the proposed CP DRA is carried out using HFSS 15.0. Several simulated parameters, including the AR, VSWR, and gain, are presented in Figs. 6–9. For brevity, only the effects of the short stub length, L_{stub}, and the vertical probe height, h_p, are presented.

To demonstrate the effect of short stub length on AR, the simulated ARs for the proposed antenna with different L_{stub} are also shown in Fig. 6. With reference to the figure, the ARs are not sensitive to the short stub length L_{stub} while they are around the order of $\lambda_g/4$. The effects on the gain and VSWR of the antenna are minimal (not shown).

The results of varying h_p are shown in Figs. 7–9. It is observed from Fig. 7 that the VSWR does not change

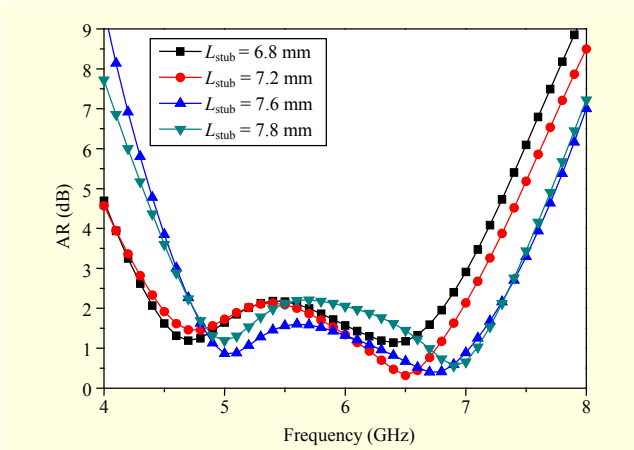

Fig. 6. Simulated ARs of antenna II for different short stub lengths.

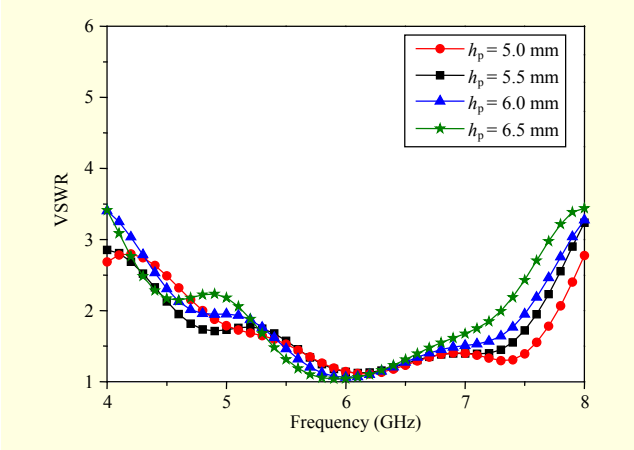

Fig. 7. Simulated VSWRs of proposed antenna for different probe heights.

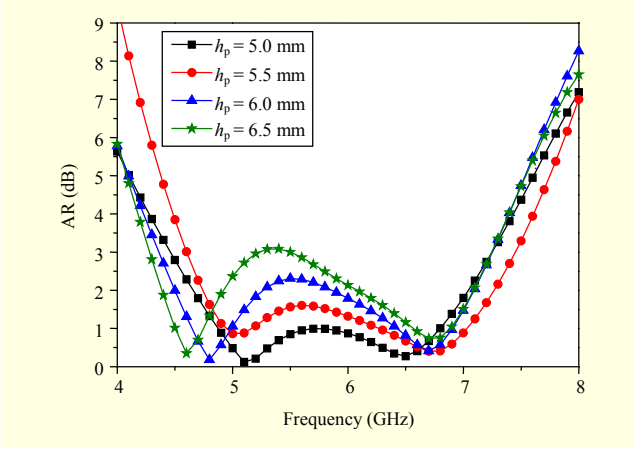

Fig. 8. Simulated ARs of proposed antenna for different probe heights.

significantly, but the impedance bandwidth deteriorates when the probe height h_p increases from 5.0 mm to 6.5 mm. The

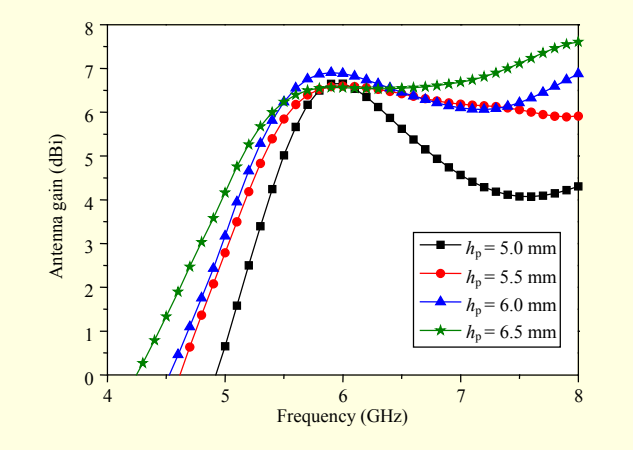

Fig. 9. Simulated gains of proposed antenna for different probe heights.

effect on AR and gain of the antenna are shown in Figs. 8 and 9, respectively. It is found that the probe height h_p does not affect the AR much, but gain bandwidth changes significantly when the height h_p increases from 5.0 mm to 6.5 mm.

It is found that the present CP antenna has stable AR characteristics. Therefore, the key problem in the design of the CP antenna is to find the tradeoff between impedance match and gain bandwidth. The optimal dimension of probe height h_p is given in Section III, of which the proposed antenna has simultaneously best impedance matching and gain bandwidth.

III. Results and Discussion

The proposed CP DRA with the WHC is designed at a central frequency of 6.0 GHz, and all simulations are based on HFSS 15.0. The dimensions of the proposed antenna are optimized. Achieving good impedance matching and gain bandwidth are the main objectives in the optimization procedure. By optimization, the final optimal dimensions are shown as follows: a = 5.1 mm, h = 9.5 mm, W_0 = 1.3 mm, W_1 = 0.71 mm, L_{stub} = 7.6 mm, W_{stub} = 0.62 mm, h_p = 5.5 mm, and r_p = 0.3 mm. A prototype of the proposed antenna is fabricated and measured for the purpose of supporting the design.

The Agilent 8719ES vector network analyzer was employed in the impedance measurement. The simulated and measured VSWRs are illustrated in Fig. 10. With reference to the figure, the measured VSWR reasonably agrees with the simulation, and a further similar three resonances are observed from the two VSWR curves. The measured result exhibits an impedance bandwidth of 52.5% from 4.5 GHz to 7.65 GHz for VSWR $\leq$ 2.

The standard linearly polarized horn antenna was employed in the measurement of radiation. The simulated and measured ARs in the broadside direction (θ = 0°) against frequency are

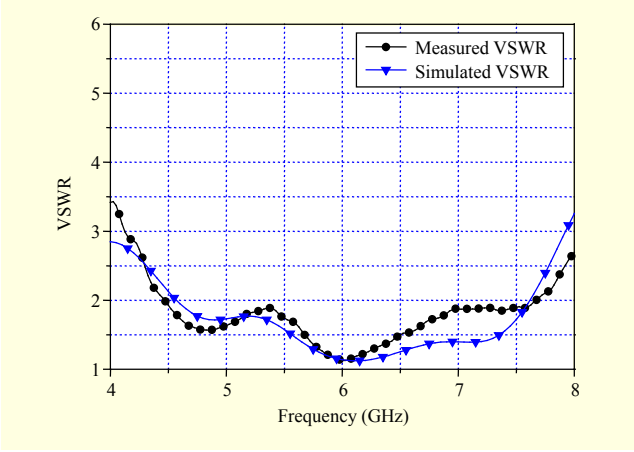

Fig. 10. Simulated and measured VSWRs.

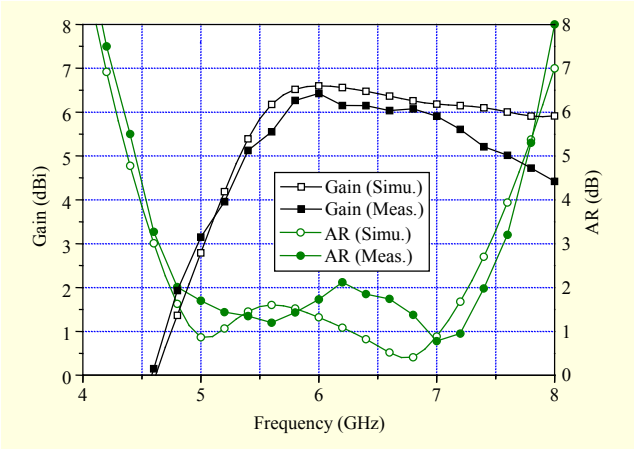

Fig. 11. Measured and simulated ARs and gains.

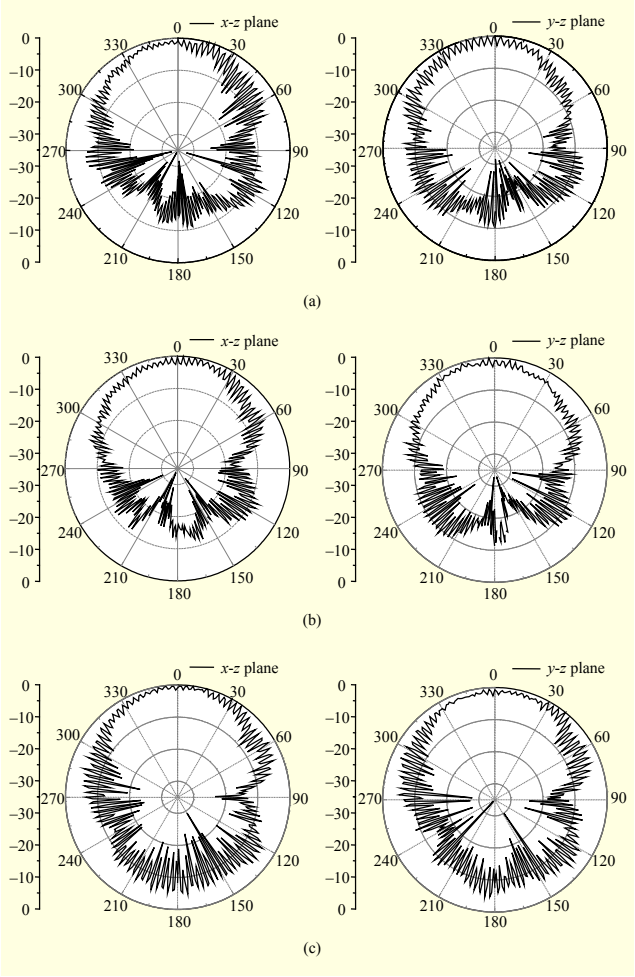

Fig. 12. Measured radiation patterns in *x*-*z* and *y*-*z* plane: (a) 5.0 GHz, (b) 6.0 GHz, and (c) 7.0 GHz.

shown in Fig. 11. The measured AR is observed with a 3 dB bandwidth of 48.66% from 4.63 GHz to 7.55 GHz. The measured and simulated antenna gains are illustrated in the same figure. The measured result shows a gain bandwidth of 44.66% from 4.97 GHz to 7.65 GHz for a gain of no less than 3 dBi, and the measured peak gain at the boresight direction is 6.4 dBi at the central frequency.

The measured radiation patterns at three frequencies, 5.0 GHz, 6.0 GHz, and 7.0 GHz, in the *x*-*z* and *y*-*z* plane are illustrated in Fig. 12. With reference to the figures, the patterns demonstrate the stable main beams and show good ARs in broadside directions over the whole passband.

Several dual/multiple-feed CP DRAs are compared with the proposed CP DRA fed by the WHC. The results reveal a significant enhancement on the AR and impedance bandwidths for the proposed CP DRA over the CP antennas in the literatures [15]–[19]. It should be mentioned that the proposed WHC achieves much wider bandwidth than those of the feed networks used in [15]–[19]; therefore, the AR and impedance bandwidths of the proposed antenna are enhanced.

IV. Conclusion

In this paper, a broadband CP DRA with a novel wideband feed network has been reported. First, the feed network WHC is proposed, which delivers good impedance matching, equal power splitting, and consistent 90° phase shift over a wide bandwidth. Second, a CP DRA with the proposed WHC is simulated, fabricated, and measured. The measured results reasonably agree with the simulations and demonstrate a significant enhancement on CP performance and impedance matching — exhibiting 3 dB AR bandwidth of 48.66% and impedance bandwidth of 52.5% for VSWR $\leq$ 2. With the simple structure and advanced performances, the proposed CP DRA with the WHC is promising for its application in C-band communication systems.

References

[1] S.A. Long, M.W. McAllister, and L.C. Shen, "The Resonant

Cylindrical Dielectric Cavity Antenna," *IEEE Trans. Antennas Propag.*, vol. 31, no. 3, May 1983, pp. 406–412.

[2] K.W. Leung, E.H. Lim, and X.S. Fang, "Dielectric Resonator Antennas: From the Basic to the Aesthetic," *Proc. IEEE*, vol. 100, no. 7, July 2012, pp. 2181–2193.

[3] A. Petosa and A. Ittipiboon, "Dielectric Resonator Antennas: A Historical Review and the Current State of the Art," *IEEE Antennas Propag. Mag.*, vol. 52, no. 5, Oct. 2010, pp. 91–116.

[4] A. Motevasselian, A. Ellgardt, and B.L.G. Jonsson, "A Circularly Polarized Cylindrical Dielectric Resonator Antenna Using a Helical Exciter," *IEEE Trans. Antennas Propag.*, vol. 61, no. 3, Mar. 2013, pp. 1439–1443.

[5] A.A. Kishk, "An Elliptic Dielectric Resonator Antenna Designed for Circular Polarization with Single Feed," *Microw. Opt. Technol. Lett.*, vol. 37, no. 6, June 2003, pp. 454–456.

[6] K.P. Esselle, "Circularly Polarised Higher-Order Rectangular Dielectric Resonator Antenna," *Electron. Lett.*, vol. 32, no. 3, Feb. 1996, pp. 150–151.

[7] G. Almpanis, C. Fumeaux, and R. Vahldieck, "Offset Cross-Slot-Coupled Dielectric Resonator Antenna for Circular Polarization," *IEEE Microw. Wireless Compon. Lett.*, vol. 16, no. 8, Aug. 2006, pp. 461–463.

[8] R. Chair et al., "Aperture-Fed Wideband Circularly Polarized Rectangular Stair-Shaped Dielectric Resonator Antenna," *IEEE Trans. Antennas Propag.*, vol. 54, no. 4, Apr. 2006, pp. 1350–1352.

[9] M.I. Sulaiman and S.K. Khamas, "A Singly Fed Rectangular Dielectric Resonator Antenna with a Wideband Circular Polarization," *IEEE Antennas Wireless Propag. Lett.*, vol. 9, June 2010, pp. 615–618.

[10] S. Jeon, H. Choi, and H. Kim, "Circular Polarization Dielectric Resonator Antenna Excited by Single Loop Feed," *ETRI J.*, vol. 31, no. 1, Feb. 2009, pp. 74–76.

[11] M. Simeoni et al., "Plastic-Based Supershaped Dielectric Resonator Antennas for Wide-Band Applications," *IEEE Trans. Antennas Propag.*, vol. 59, no. 12, Dec. 2011, pp. 4820–4825.

[12] Y.-M. Pan and K.W. Leung, "Wideband Circularly Polarized Dielectric Bird-Nest Antenna with Conical Radiation Pattern," *IEEE Trans. Antennas Propag.*, vol. 61, no. 2, Feb. 2013, pp. 563–570.

[13] M. Khalily, M.R. Kamarudin, and M.H. Jamaluddin, "A Novel Square Dielectric Resonator Antenna with Two Unequal Inclined Slits for Wideband Circular Polarization," *IEEE Antennas Wireless Propag. Lett.*, vol. 12, Sept. 2013, pp. 1256–1259.

[14] R.K. Mongia et al., "Circularly Polarized Dielectric Resonator Antenna," *Electron. Lett.*, vol. 30, no. 17, Aug. 1994, pp. 1361–1362.

[15] K.W. Leung et al., "Circular Polarized Dielectric Resonator Antenna Excited by Dual Conformal Strips," *Electron. Lett.*, vol. 36, no. 6, May 2000, pp. 484–486.

[16] K.-W. Khoo, Y.-X. Guo, and L.C. Ong, "Wideband Circularly Polarized Dielectric Resonator Antenna," *IEEE Trans. Antennas Propag.*, vol. 55, no. 7, July 2007, pp. 1929–1932.

[17] B. Li, C.-X. Hao, and X.-Q. Sheng, "A Dual-Mode Quadrature-Fed Wideband Circularly Polarized Dielectric Resonator Antenna," *IEEE Antennas Wireless Propag. Lett.*, vol. 8, Aug. 2009, pp. 1036–1038.

[18] E.H. Lim, K.W. Leung, and X.S. Fang, "The Compact Circularly Polarized Hollow Rectangular Dielectric Resonator Antenna with an Underlaid Quadrature Coupler," *IEEE Trans. Antennas Propag.*, vol. 59, no. 1, Jan. 2011, pp. 288–293.

[19] X.S. Fang and K.W. Leung, "Linear-/Circular-Polarization Designs of Dual-/Wide-Band Cylindrical Dielectric Resonator Antennas," *IEEE Trans. Antennas Propag.*, vol. 60, no. 6, June 2012, pp. 2662–2671.

[20] D.M. Pozar, "*Power Dividers and Directional Couplers*," *Microw. Eng.*, 4th ed., Hoboken, NJ, USA: John Wiley & Sons, 2012, pp. 363–367.

[21] A.A. Kishk, "Performance of Planar Four-Element Array of Single-Fed Circularly Polarized Dielectric Resonator Antenna," *Microw. Opt. Technol. Lett.*, vol. 38, no. 5, Sept. 2003, pp. 381–384.

[22] S.-Y. Eom and H.-K. Park, "New Switched-Network Phase Shifter with Broadband Characteristics," *Microw. Opt. Technol. Lett.*, vol. 38, no. 4, Aug. 2003, pp. 255–257.

Ru-Ying Sun received her BS degree in electronic engineering from Ludong University, Yantai, China, in 2003 and her MS degree in information and communication engineering from Chongqing University, China, in 2006. She is currently pursuing her PhD degree in information and communication engineering at Wuhan University, China. Since July of 2006, she has worked with the Department of Electrical Engineering, Linyi University, China. Her research interests include antennas, microwave circuits, and wireless communications.